

Description of Remote Sensing Systems Version-7 Geophysical Retrievals

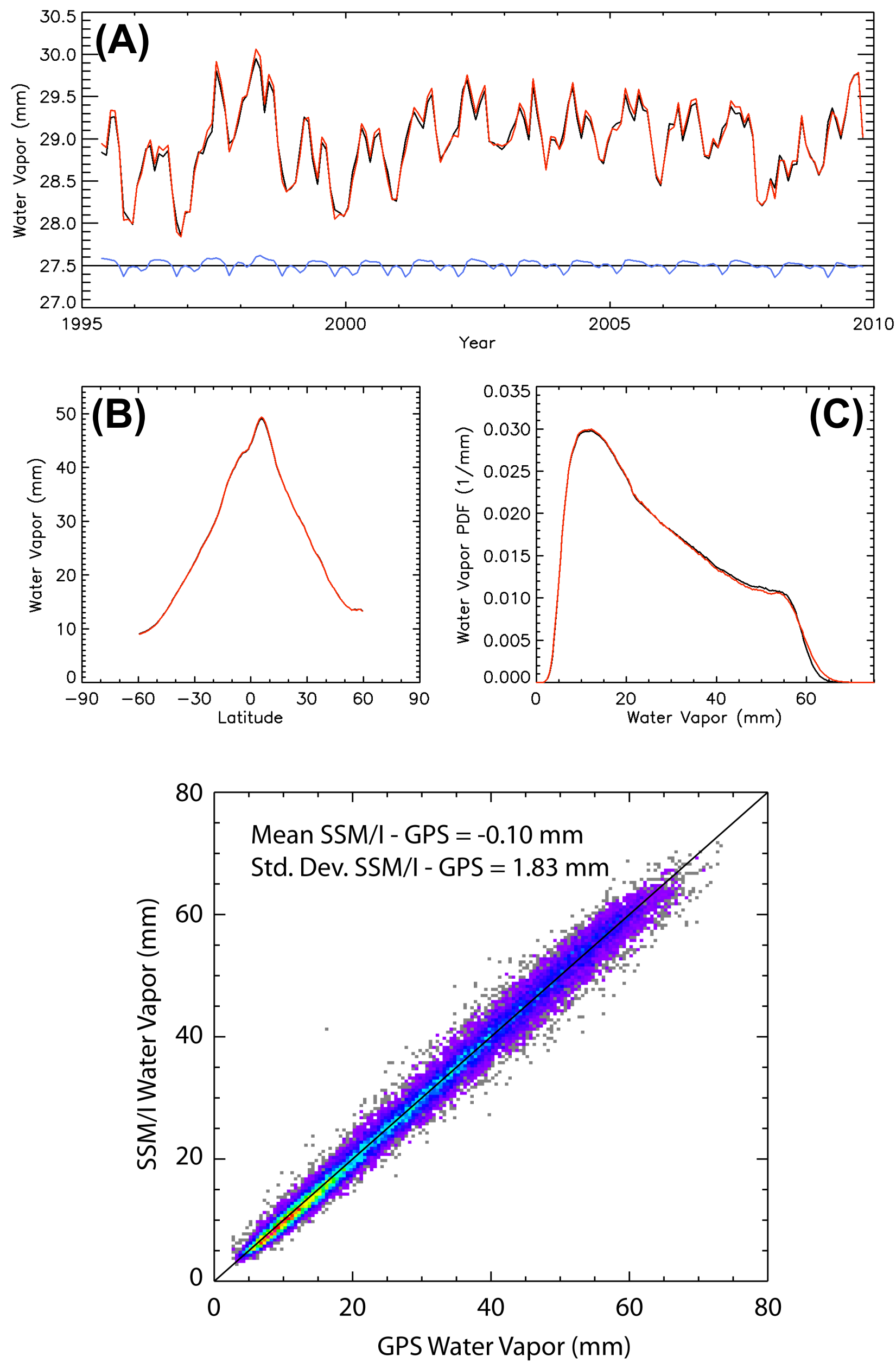
Kyle Hilburn, Frank Wentz, Carl Mears, Thomas Meissner, and Deborah Smith

hilburn@remss.com

Remote Sensing Systems
www.remss.com

The purpose of this poster is to briefly describe the major changes to Remote Sensing Systems (RSS) Version-7 (V7) microwave radiometer processing and demonstrate the impact of these changes on the retrieved geophysical parameters. There are three major changes in V7 processing: (1) the water vapor continuum absorption model was re-derived, (2) the clear-sky bias in cloud water was removed and the data format for cloud water was changed, (3) the beamfilling correction in the rain algorithm was modified.

We have released V7 data for F16 SSMIS and will soon be releasing F17 SSMIS. We will also be releasing V7 data for WindSat, SSM/I (F08, F10, F11, F13, F14, and F15), AMSR-E, and TMI. This poster uses F13 SSM/I to illustrate the impact of the algorithm changes on retrievals. All statistics are calculated for the F13 time period of May 1995 through October 2009.



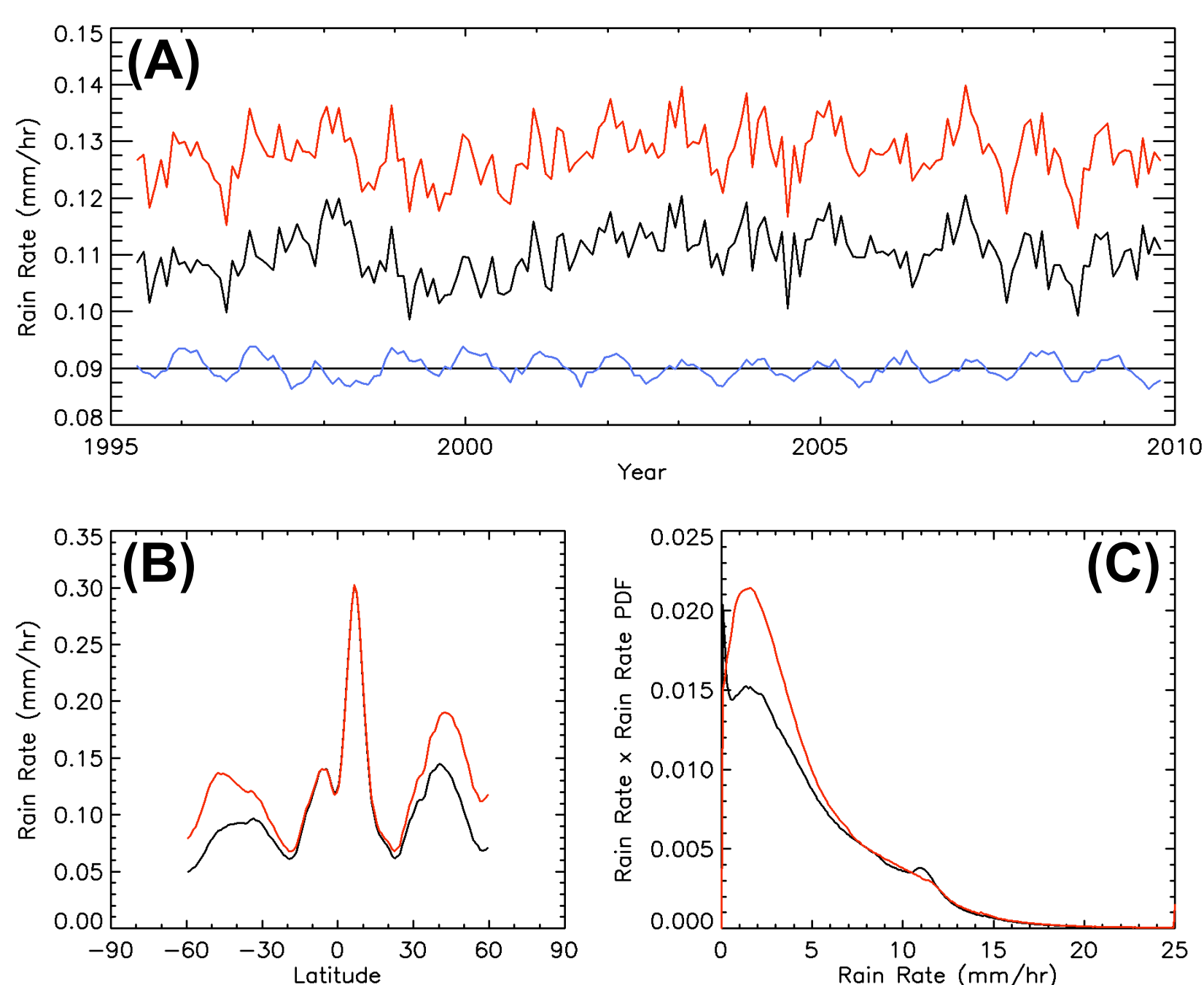
WATER VAPOR summary for V6 (black) and V7 (red) is shown to the LEFT. Panel (A) shows global mean time series and the V7-V6 (blue) difference time series offset from zero by 27.5 mm. Panel (B) shows zonal averages. Panel (C) shows probability distribution functions.

The global mean water vapor has changed by less than 0.1% between V7 (28.992 mm) and V6 (28.974 mm). V7 vapor retrievals are very similar to V6 except that, as Panel (C) shows, V7 has slightly higher vapors for values above 55 mm due to changes in the water vapor continuum absorption.

The V6 processing used the vapor absorption model of Wentz and Meissner (2000) and the oxygen absorption model of Rosenkranz (1998). The vapor absorption model for V7 was re-derived by analyzing WindSat and SSM/I brightness temperatures as a function of V6 SSM/I water vapor. For the derivation, V6 SSM/I retrievals were used in the radiative transfer model, and cloud water was lowered by 0.008 mm to remove the clear sky bias in V6 cloud water (Horvath and Gentemann, 2007). The water vapor continuum absorption was changed, but the shape and strength of the 22 GHz water vapor absorption line were not modified. Adjustments were made to coefficients of both the foreign-broadened and self-broadened water vapor continuum absorption to obtain the best fit between measured brightness temperatures and radiative transfer model computed brightness temperatures. Comparing the V7 vapor absorption model against Rosenkranz (1998), the foreign-broadened continuum is increased by 10% and the self-broadened continuum is reduced by a factor of $0.375 \times \text{frequency}(\text{GHz})^{0.15}$. The new continuum model in V7 is very close to the continuum model in the latest version of MonoRTM.

The changes to the vapor absorption model have the effect of increasing vapor in the range 50-60 mm by about 1%, and increasing vapor above 60 mm by about 2-3%. The V7 SSM/I water vapor retrievals agree better with GPS-derived water vapor at high vapor values based on 14 ground-based GPS stations on small islands providing roughly 30K collocations (Figure to LEFT).

CLOUD WATER has changed in V7 to remove the 0.008 mm clear sky bias in our V6 cloud retrievals (Horvath and Gentemann, 2007). The bias was removed at the calibration stage by lowering the cloud water entering into the radiative transfer model. While cloud water is physically a non-negative quantity, random errors in brightness temperatures produce negative cloud retrievals. In V6, we set these negative values to zero, which can produce a biased estimate. In V7, we are providing the negative cloud values, which has resulted in a **change to our data format**. For V6, cloud liquid water was obtained by scaling the byte value (0-250) by 0.01 to get values between 0-2.5 mm. For V7, the byte value (0-250) is first scaled by 0.01 and then **offset by -0.05 mm** to get values between -0.05-2.45 mm. Negative cloud values account for roughly 9% of the data and produce a 2% effect on the mean rain-free cloud water.



RAIN RATE summary for V6 (black) and V7 (red) is shown to the LEFT. Panel (A) shows global mean time series and the V7-V6 (blue) difference time series offset from zero by 0.09 mm/hr with the mean bias of 0.0177 mm/hr removed. Panel (B) shows zonal averages. Panel (C) shows probability distribution functions times rain rate. Thus, the area under the curve in Panel (C) gives the average rain rate.

The largest differences between V6 and V7 are in the rain rate retrievals. The global mean rain rate for V7 (0.1278 mm/hr) has increased by 16% over V6 (0.1101 mm/hr). The increase in V7 rain rates comes from changes in the extratropical values. Zonal averages (Panel B) show that in the tropics V7 agrees with V6 to within 1%; while the northern hemisphere is 27% higher in V7 and the southern hemisphere is 37% higher. The increase in extratropical rain rates is due to the changes in the beamfilling correction for V7. The changes smoothed the discontinuity in the correction for rain rates near zero, which had caused a spike in the V6 rain PDF (Panel C). In addition to smoothing the spike, the new beamfilling correction gave V7 a greater contribution to the mean from light rain rates less than 5 mm/hr.

Prior to V6, rain retrievals were made with the Wentz and Spencer (1998) rain algorithm. In this algorithm, the beamfilling correction depends only on the 19 and 37 GHz attenuation values, responding mainly to their ratio. Using high resolution AMSR-E data to simulate lower resolution SSM/I data, Hilburn and Wentz (2008) found two problems with that approach. First, the correction did not properly account for saturation of the 37 GHz channel, thus overestimating the amount of beamfilling correction. Second, the correction did not explicitly account for sensor resolution. Hilburn and Wentz (2008) modified the beamfilling correction to depend on the footprint size, in accordance with their simulated results. Thus, the V6 beamfilling correction has two parts: one part that depends on the 19-to-37 GHz attenuation ratio and a second part that depends on the footprint size. Unfortunately, the way the beamfilling correction was implemented in V6 caused jumps in the beamfilling correction to occur. Because of the footprint size dependence, the V6 beamfilling correction was always slightly larger than one, with the value depending on the sensor. The discontinuities in the V6 correction would occur at the no-rain/rain boundary and at the point where the attenuation ratio suddenly becomes greater than the theoretical value for spatially uniform rain. These jumps were fixed in V7 by smoothly turning-on the beamfilling correction. This has caused the V7 rain retrievals to have more beamfilling correction applied (especially at light rain rates) than V6, and has resulted in increased extratropical rain rates. The higher extratropical rain rates are more consistent with the global water cycle balance (Wentz et al., 2007).